JACS
JOURNAL OF THE AMERICAN CHEMICAL SOCIETY
pubs.acs.org/JACS
Communication

Reactivity of a Gold-Aluminyl Complex with Carbon Dioxide: A Nucleophilic Gold?

Diego Sorbelli,*,$ Leonardo Belpassi,*,$ and Paola Belanzoni*,$

Cite This: J. Am. Chem. Soc. 2021, 143, 14433−14437

ABSTRACT: A gold-aluminyl complex has been recently reported to feature an unconventional gold nucleophilic center, which was revealed through reactivity with carbon dioxide leading to the Au-CO_2 coordination mode. In this work, we computationally investigate the reaction mechanism, which is found to be cooperative, with the gold−aluminum bond being the actual nucleophile and Al also behaving as electrophile. The Au−Al bond is shown to be mainly of an electron-sharing nature, with the two metal fragments displaying a diradical-like reactivity with CO_2.

Recently, a striking reactivity of CO_2 with a complex bearing a Au−Al bond has been reported.[1] A combination of the new generation aluminyl anion[2] [K{Al(NON)}]$_2$ with a phosphine gold ^{t}Bu$_3$PAuI affords the [^{t}Bu$_3$PAuAl(NON)] complex (**I**) which, in reaction with CO_2 (1 atm at room temperature in toluene), leads to the stable [^{t}Bu$_3$PAuCO$_2$Al-(NON)] complex (**II**), where Au binds to the CO_2 carbon atom (Scheme 1). This CO_2 coordination mode has been considered

Scheme 1. Examples of Nucleophilic Gold (I),[1] Copper (III, V),[7] and Amido-Digermyne (VII)[12] Compounds and Their CO_2 Insertion Reaction Products (II, IV, VI, and VIII)

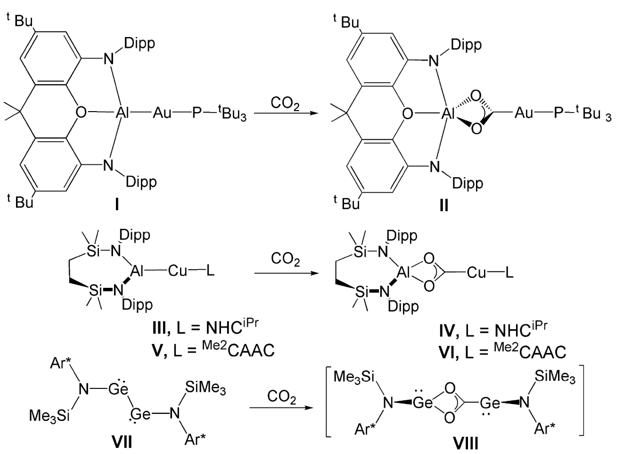

as the revealing of an unconventional nucleophilic behavior of gold, which, in contrast, is well-known to be an extremely powerful electrophile in organic reactions involving unsaturated CC bonds.[3] The authors suggested that the aluminyl anion [Al(NON)]$^-$ is able to induce an extremely polarized Au(δ-)-Al(δ+) bond, with a significant negative charge at the gold site, which is able to reverse its reactivity. DFT calculations combined with quantum theory of atoms in molecules (QTAIM) charge analysis have shown a substantial electron transfer from [Al(NON)]$^-$ to [^{t}Bu$_3$PAu]$^+$ (1.56 electrons) and a negative charge at Au (−0.82).[1] This picture seems to be consistent with the difference in electronegativity values of the two metals (Au = 2.54, Al = 1.61 on the Pauling scale) and with the relativistic effects on gold which stabilize and contract the 6s orbital,[4] resulting in the gold highest electron affinity (2.30 eV) among transition metals (other coinage metals have considerably smaller values, Cu 1.23 eV; Ag 1.30 eV).[5] Complex **I** is not the only complex in which Au would act as a nucleophile toward polar multiple bond.[6] Two copper-aluminyl complexes (**III** and **V** in Scheme 1) have been reported to insert CO_2 into the Cu−Al bond, resulting in complexes **IV** and **VI** (Scheme 1), which are very much similar to complex **II** in terms of structure and kinetic stability.[7] A significant covalency of the Al−Cu bond and only slightly negative charges on Cu (e.g., −0.09 in **III**) have been calculated, revealing here only a small polarization of the M(δ-)-Al(δ+) bond.

In addition to strongly polarized M(δ-)-Al(δ+) bonds in heterodinuclear complexes,[8] CO_2 activation by homodinuclear main-group element species,[9,10] including diradicals,[11] is not uncommon. Frenking and Jones[12] demonstrated that the facile reduction of CO_2 to CO by a symmetric amido-digermyne compound (**VII**) proceeds through an asymmetrical intermediate (**VIII**) that bears a structural analogy with complex **II**.

The similar coordination modes of CO_2 in the Au−Al, Cu−Al, and Ge−Ge bonds is eye-catching, in view of the different degrees of polarization of the insertion metal−metal site, which is expected to determine the effectiveness of the metal nucleophilic behavior. This prompted us to computationally investigate the mechanism of the CO_2 insertion into the pioneering nucleophilic [^{t}Bu$_3$PAuAl(NON)] complex which has not been explored yet and the actual nucleophilic ability of

Received: June 29, 2021
Published: September 2, 2021

https://doi.org/10.1021/jacs.1c06728
J. Am. Chem. Soc. 2021, 143, 14433−14437

Au in this "unorthodox reaction ".[13] We demonstrate that the nucleophilic attack is actually performed by the Au−Al σ bond, revealing a bimetallic (Au/Al) cooperation in the CO_2 binding. The attack is also assisted by a secondary interaction, involving the partially empty $3p_x$ atomic orbital of Al, which exploits its Lewis acidity. Transition state and intermediate structures found here suggest a radical-like insertion of CO_2 in the Au−Al bond, which has been consistently shown to have an electron-sharing character.

The free energy profile for the CO_2 insertion into the Au−Al bond of **I** was calculated using density functional theory (DFT) with the inclusion of relativistic effects, solvation, and dispersion interactions (see SI for computational details), and it is shown in Figure 1. Complex **I** was slightly simplified at the NON site

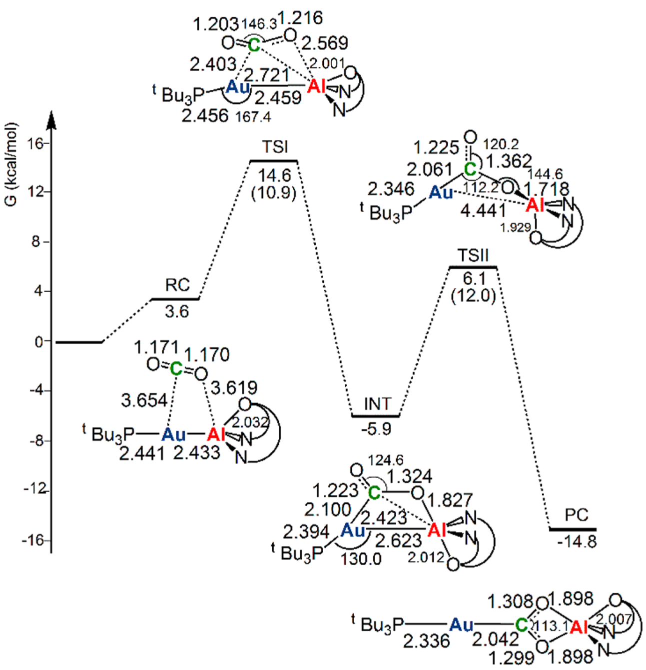

Figure 1. Free energy reaction profile for the CO_2 insertion into the Au−Al bond in the [^{t}Bu$_3$PAuAl(NON')] complex. Δ*G* values refer to the energy of the separated reactants taken as zero. Activation free energy barriers are reported in parentheses. Selected interatomic distances (Å) and bond angles (degrees) are given with the molecular structures.

(denoted as NON'). The modeling effect is evaluated in Table S1. The optimized geometries of [^{t}Bu$_3$PAuAl(NON')], RC, TSI, INT, TSII, and [^{t}Bu$_3$PAuCO$_2$Al(NON')] (PC) complexes are reported in the SI (Figure S1) and show good agreement with available experimental data (Figure S2 and Table S2).

The nucleophilic attack to the CO_2 carbon atom has a relatively low activation free energy barrier ($\Delta G^{\#}$ = 10.9 kcal/mol). At the TSI, the carbon atom of CO_2 is both very close to Au (2.403 Å) and at a relatively short distance from Al (2.721 Å), and a substantial bending of CO_2 and asymmetry between the two C−O bonds are also observed (see Table S3 for the evolution of the most relevant Mayer's bond orders along the reaction path). Subsequent complete bonding of CO_2 carbon atom to Au and oxygen atom to Al leads to the formation of intermediate INT, which is stabilized by 20.5 kcal/mol. As a result, the Au−Al bond distance slightly increases and the ^{t}Bu$_3$PAu moiety coordinates almost linearly with the carbon atom of CO_2. A second transition state (TSII) is located with an activation free energy barrier $\Delta G^{\#}$ of 12.0 kcal/mol, showing a substantial breaking of the Au−Al bond. Finally, the oxygen atom of CO_2 attack to the electrophilic Al center leads to the thermodynamically stable product complex PC. The overall CO_2 insertion into the Au−Al bond is exergonic by −14.8 kcal/mol.

To get insights into the nature of the CO_2 insertion process, we analyze the first activation barrier using the Activation Strain Model (ASM)[14−16] (main results in Figure 2, left panel). The ASM formalism is briefly summarized in the SI, and all the results are reported in Table S4.

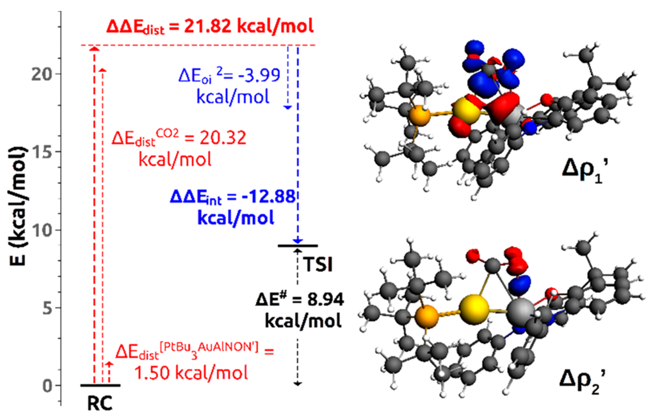

Figure 2. Activation Strain Model (ASM) decomposition of the electronic energy activation barrier $\Delta E^{\#}$ (left) (see text). Isodensity surfaces (2 me/a_0^3) for the NOCV deformation density maps (charge flux is red → blue) corresponding to the $\Delta\rho_1$' (top right) and $\Delta\rho_2$' (bottom right) contributions to the CO_2-[^{t}Bu$_3$PAuAl(NON')] fragments interaction in the transition state TSI.

The distortion energy contribution ($\Delta\Delta E_{dist}$ = 21.82 kcal/mol) to the electronic energy activation barrier ($\Delta E^{\#}$=8.94 kcal/mol) is almost completely associated with the CO_2 bending (20.32 kcal/mol, see Table S5), whereas the stabilizing interaction contribution ($\Delta\Delta E_{int}$= −12.88 kcal/mol) mainly arises from the orbital interaction energy at TSI (−53.30 kcal/mol) (see Table S6). The results of the ETS-NOCV[17] method coupled with the Charge Displacement (CD) Analysis[18] (see SI for methodological details) are summarized below. In Figure 2 (right panel), the two most important components ($\Delta\rho_1$' and $\Delta\rho_2$') of the total deformation density are shown.

The main interaction component ($\Delta\rho_1$') is clearly characterized by an electron density depletion localized on both Au and Al atoms and by an electron density accumulation at the CO_2 site. This component is associated with a significant energy stabilization (−41.20 kcal/mol) and a charge transfer from the Au−Al bond region to carbon dioxide of 0.326 e. The decomposition into the donor and acceptor NOCV orbitals[19] (Figure S3) shows that the electron density accumulation has the main contribution from the LUMO of CO_2, while the electron density depletion shows contributions from the HOMO−2 and HOMO of the [^{t}Bu$_3$PAuAl(NON')] fragment, both representing the Au−Al σ bond, where Al $3s3p_z$−Au $6s6p_z$ type orbitals are involved. Component $\Delta\rho_2$' reveals an electron density accumulation at the Al center (note that its shape recalls that of an atomic p_x orbital), coming from one of the oxygen atoms of CO_2. Decomposition into donor and acceptor NOCV orbitals (Figure S4) shows that the main contribution to the donor orbital is the HOMO of CO_2, whereas a clear characterization of the acceptor orbital is less straightforward,

https://doi.org/10.1021/jacs.1c06728
J. Am. Chem. Soc. 2021, 143, 14433−14437

since several delocalized unoccupied MOs, all with small Al $3p_x$ orbital mixing, contribute to it. The $\Delta\rho_2'$ contribution is not negligible: 0.047 e are transferred toward Al from CO_2, with an associated orbital interaction energy of −3.99 kcal/mol (which notably accounts for one-third of the interaction stabilization to the activation barrier $\Delta\Delta E_{int}$).

The reaction mechanism in Figure 1 bears surprising analogies with the first steps of the reaction profile for the reduction of CO_2 to CO by [LGe-GeL] (see Figure 3 of ref 12), although complex **II** does not evolve to CO elimination (the resulting oxide complex [^{t}Bu$_3$PAuOAl(NON′)][CO] has been calculated to be highly unstable with ΔG = 29.8 kcal/mol). The high reactivity of digermynes has been often attributed to the nonnegligible biradical character in these systems.[11,19,20] A possible diradicaloid character of the Au−Al bond in the [^{t}Bu$_3$PAuAl(NON)] complex is certainly very intriguing. Remarkably, the coordination modes of CO_2 in the separated neutral open shell doublet [^{t}Bu$_3$PAu(CO_2)]· and [CO_2Al-(NON′)]· fragments closely match those found at the TSI and INT (Figures S5, S6 and discussion therein). This prompted us to review the Au−Al bond nature in complex **I**. We carry out the CD-NOCV analysis on the [^{t}Bu$_3$PAuAl(NON′)] complex by choosing the open-shell radical fragments [^{t}Bu$_3$PAu]· and [(NON′)Al]· on the basis of EDA analysis[21] using different fragmentations (Table S7 and ref 22). The main results of the CD-NOCV analysis are reported in Figure 3.

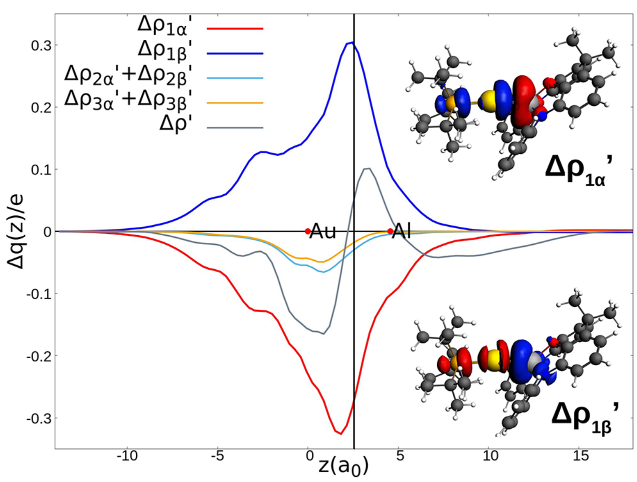

Figure 3. Charge Displacement (CD-NOCV) curves for the interaction between doublet [^{t}Bu$_3$PAu]· and [(NON′)Al]· fragments in the [^{t}Bu$_3$PAuAl(NON′)] complex. Red dots indicate the position of the nuclei along the z axis. The vertical solid line marks the isodensity boundary between the fragments. Positive (negative) values of the curve indicate right-to-left (left-to-right) charge transfer (see Supporting Information for details). Insets: isodensity surfaces (1 me/a_0^3) of the two NOCV deformation densities $\Delta\rho_{1\alpha}'$ (top, right) and $\Delta\rho_{1\beta}'$ (bottom, right) (charge flux is red → blue).

The CD-NOCV curves clearly exhibit two similar main charge fluxes in opposite directions, which consist of an electron transfer from Au toward Al ($\Delta\rho_{1\alpha}'$, red curve and inset in Figure 3) and from Al toward Au ($\Delta\rho_{1\beta}'$, blue curve and inset in Figure 3). These two charge fluxes have also similar CT absolute values (0.272 and 0.299 e for $\Delta\rho_{1\alpha}'$ and $\Delta\rho_{1\beta}'$, respectively), associated orbital interaction energies (−32.66 and −24.49 kcal/mol for $\Delta\rho_{1\alpha}'$ and $\Delta\rho_{1\beta}'$, respectively), and NOCV eigenvalues (0.45 and 0.42 for $\Delta\rho_{1\alpha}'$ and $\Delta\rho_{1\beta}'$, respectively) as shown in Table S8. Other contributions to the Au−Al bond (CD-NOCV curves labeled as $\Delta\rho_{2\alpha}' + \Delta\rho_{2\beta}'$ and $\Delta\rho_{3\alpha}' + \Delta\rho_{3\beta}'$) describe the π back-donations (see Figure S7) and are definitely smaller in magnitude. The CD curve associated with the total deformation density ($\Delta\rho'$) shows an almost symmetric charge accumulation at the bonding region with a slightly positive CT (0.05 e) going from the radical [(NON′)Al]· to [^{t}Bu$_3$PAu]·, which can be associated with the net polarization of the Au−Al bond. To definitely assess the electron-sharing bond nature, the CD-NOCV analysis for a nonpolar covalent bond system, such as the homonuclear Au_2 molecule, is presented in Figures S8, S9 for comparison. The CD-NOCV curves in Figure 3 and Figure S8 are indeed very similar.

We also find that this bonding scheme is not peculiar of the Au−Al bond in [^{t}Bu$_3$PAuAl(NON′)]. A qualitatively analogous picture has been also obtained for two complexes with a Cu−Al bond, i.e., a model [^{t}Bu$_3$PCuAl(NON′)] (where we substituted gold with copper and reoptimized the structure) and the experimental complex **III**.[7] (see Tables S9, S10 and Figures S10, S11; for a comparative EDA, see Table S11). Before concluding, we comment on the two main theoretical points which suggested in ref 1 the formation of a strongly polarized Au−Al bond with a large negative charge on Au, i.e., (i) the Au/Al difference in the *atomic* electronegativity values and (ii) the *atomic* charge on Au. Concerning point (i), although the large Au/Al atomic electronegativity difference (0.93 on the Pauling scale, 2.12 (calculated) and 2.19 (experimental) on the Mulliken scale (see Table S12) seems to be inconsistent with an electron-sharing bond, the calculated Mulliken "molecular electronegativity" is practically identical (2.56 vs 2.53 eV for [^{t}Bu$_3$PAu]· and [Al(NON′)]·, respectively) (Table S13). For point (ii), the atomic charges show a huge variability range with the chosen method (consistently with the highly directional and diffuse HOMO of the aluminyl anion, Figure S12): q^{Au}, from −0.83 to +0.22; q^{Al}, from 2.18 to 0.18 (Table S14) which makes an assessment of the bond polarization based on these numbers impossible.

In summary, the reactivity shown here points out that both Au and Al centers act as nucleophiles (radical-like mechanism), with the electrophilic behavior of Al also assisting the interaction with CO_2. The Au−Al bonding picture in [^{t}Bu$_3$PAuAl(NON)] is consistent with an Au(0) involved in an electron-sharing bond-type. An important general conclusion is that the reactivity of metal-aluminyl complexes with CO_2 resulting in M-CO_2 coordination mode cannot be considered in itself as a probe for a strongly polarized M(δ-)-Al(δ+) bond and for the metal behaving as a standard nucleophilic center. We believe that the interpretative framework given here may be useful for future experimental investigations on CO_2 capture and reduction by these unconventional bimetallic complexes.

■ ASSOCIATED CONTENT

Supporting Information

The Supporting Information is available free of charge at https://pubs.acs.org/doi/10.1021/jacs.1c06728.

Methodology and computational details; optimized geometries; Mayer's bond order along the path; Activation Strain Model and EDA results; donor and acceptor NOCV orbital decomposition; analysis of the [(NON′)Al] and [^{t}Bu$_3$PAu] fragments; selection of fragmentations for bonding analysis; CD-NOCV analysis complete results; CD-NOCV and EDA analysis of [^{t}Bu$_3$PCuAl(NON′)] and [NHC^{iPr}CuAlSiN^{Dipp}] com-

https://doi.org/10.1021/jacs.1c06728
J. Am. Chem. Soc. 2021, 143, 14433−14437

plexes; Au, Al, and "molecular" ionization energy and electron affinity; AIM, Mulliken, Hirshfeld, VDD, Multipole Derived, CM5 calculated atomic charges on Au and Al; [(NON')Al] HOMO electron density map (PDF)

■ AUTHOR INFORMATION

Corresponding Authors

Diego Sorbelli — *Department of Chemistry, Biology and Biotechnology, University of Perugia, 06123 Perugia, Italy*; Email: diegosorbelli00@gmail.com

Leonardo Belpassi — *Istituto CNR di Scienze e Tecnologie Chimiche "Giulio Natta" (CNR-SCITEC), 06123 Perugia, Italy; Computational Laboratory for Hybrid/Organic Photovoltaics (CLHYO) c/o Istituto CNR di Scienze e Tecnologie Chimiche "Giulio Natta" (CNR-SCITEC), 06123 Perugia, Italy*; orcid.org/0000-0002-2888-4990; Email: leonardo.belpassi@cnr.it

Paola Belanzoni — *Department of Chemistry, Biology and Biotechnology, University of Perugia, 06123 Perugia, Italy; Istituto CNR di Scienze e Tecnologie Chimiche "Giulio Natta" (CNR-SCITEC), 06123 Perugia, Italy*; orcid.org/0000-0002-1286-9294; Email: paola.belanzoni@unipg.it

Complete contact information is available at:
https://pubs.acs.org/10.1021/jacs.1c06728

Author Contributions

$^{\$}$D.S., L.B., and P.B. contributed equally to this paper

Author Contributions

The manuscript was written through contributions of all authors. All authors have given approval to the final version of the manuscript. All authors contributed equally.

Notes

The authors declare no competing financial interest.

■ ACKNOWLEDGMENTS

This work was supported by the Ministero dell'Università e della Ricerca (MUR, project AMIS, through the program "Dipartimenti di Eccellenza −2018-2022″) and the University of Perugia ("Fondo Ricerca di Base 2019″, P.B.).

■ ABBREVIATIONS

NON	4,5-bis(2,6-diisopropylanilido)-2,7-di*tert*-butyl-9,9-dimethylxanthene
NHC^{IPr}	*N*,*N*′-di-isopropyl-4,5-dimethyl-2-ylidene
$^{Me2}CAAC$	1-((2,6-di-isopropylphenyl)-3,3,5,5-tetramethyl-pyrrolidin-2-ylidene)
SiN^{Dipp}	$(CH_2SiMe_2NDipp)_2$
Ar*	$C_6H_2\{C(H)Ph_2\}_2Me$-2,6,4.

■ REFERENCES

(1) Hicks, J.; Mansikkamäki, A.; Vasko, P.; Goicoechea, J. M.; Aldridge, S. A nucleophilic gold complex. *Nat. Chem.* **2019**, *11*, 237−241.

(2) Hicks, J.; Vasko, P.; Goicoechea, J. M.; Aldridge, S. The aluminyl anion: a new generation of aluminium nucleophile. *Angew. Chem., Int. Ed.* **2021**, *60*, 1702−1713.

(3) (a) Obradors, C.; Echavarren, A. M. Intriguing mechanistic labyrinths in gold(I) catalysis. *Chem. Commun.* **2014**, *50*, 16−28. (b) Wang, Y.-M.; Lackner, A. D.; Toste, F. D. Development of catalysts and ligands for enantioselective gold catalysis. *Acc. Chem. Res.* **2014**, *47*, 889−901. (c) Hashmi, A. S. K. Dual gold catalysis. *Acc. Chem. Res.* **2014**, *47*, 864−876. (d) Zhang, L. A non-diazo approach to α-oxo gold carbenes via gold-catalyzed alkyne oxidation. *Acc. Chem. Res.* **2014**, *47*, 877−888.

(4) Schwerdtfeger, P. Relativistic and electron-correlation contributions in atomic and molecular properties: benchmark calculations on Au and Au_2. *Chem. Phys. Lett.* **1991**, *183*, 457−463.

(5) Andersen, T.; Haugen, H. K.; Hotop, H. Binding energies in atomic negative ions: III. *J. Phys. Chem. Ref. Data* **1999**, *28*, 1511−1533.

(6) Suzuki, A.; Guo, X.; Lin, Z.; Yamashita, M. Nucleophilic reactivity of the gold atom in a diarylborylgold(I) complex toward polar multiple bonds. *Chem. Sci.* **2021**, *12*, 917−928.

(7) Liu, H.-Y.; Schwamm, R. J.; Hill, M. S.; Mahon, M. F.; McMullin, C. L.; Rajabi, N. A. Ambiphilic Al-Cu bonding. *Angew. Chem., Int. Ed.* **2021**, *60*, 14390−14393. Note that the Al-Cu complexes reported here are referred as "alumanyl".

(8) Escomel, L.; Del Rosal, I.; Maron, L.; Jeanneau, E.; Veyre, L.; Thieuleux, C.; Camp, C. Strongly polarized iridium $^{\delta-}$ - aluminium $^{\delta+}$ pairs: unconventional reactivity patterns including CO_2 cooperative reductive cleavage. *J. Am. Chem. Soc.* **2021**, *143*, 4844−4856.

(9) Stoy, A.; Böhnke, J.; Jiménez-Halla, J. O. C.; Dewhurst, R. D.; Thiess, T.; Braunschweig, H. CO_2 binding and splitting by boron-boron multiple bonds. *Angew. Chem., Int. Ed.* **2018**, *57*, 5947−5951.

(10) Weetman, C.; Bag, P.; Szilvási, T.; Jandl, C.; Inoue, S. CO_2 fixation and catalytic reduction by a neutral aluminium double bond. *Angew. Chem., Int. Ed.* **2019**, *58*, 10961−10965.

(11) Hinz, A.; Schulz, A.; Villinger, A. Metal-free activation of hydrogen, carbon dioxide, and ammonia by the open-shell singlet biradicaloid $[P(\mu\text{-NTer})]_2$. *Angew. Chem., Int. Ed.* **2016**, *55*, 12214−12218.

(12) Li, J.; Hermann, M.; Frenking, G.; Jones, C. The facile reduction of carbon dioxide to carbon monoxide with an amido-digermyne. *Angew. Chem., Int. Ed.* **2012**, *51*, 8611−8614.

(13) Bourissou, D. Changing the gold standard. *Nat. Chem.* **2019**, *11*, 199−203. This work also emphasizes the high relevance of a computational study on the gold-aluminyl complex I by an explicit request (″Density functional theory calculations would be very welcome to shed light on the mechanism of this unorthodox reaction ".).

(14) Fernández, I.; Bickelhaupt, F. M. The activation strain model and molecular orbital theory: understanding and designing chemical reactions. *Chem. Soc. Rev.* **2014**, *43*, 4953−4967.

(15) Bickelhaupt, F. M.; Houk, K. N. Analyzing reaction rates with the distortion/interaction-activation strain model. *Angew. Chem., Int. Ed.* **2017**, *56*, 10070−10086.

(16) Vermeeren, P.; van der Lubbe, S. C. C.; Fonseca Guerra, C.; Bickelhaupt, F. M.; Hamlin, T. A. Understanding chemical reactivity using the activation strain model. *Nat. Protoc.* **2020**, *15*, 649−667.

(17) Mitoraj, M. P.; Michalak, A.; Ziegler, T. A combined charge and energy decomposition scheme for bond analysis. *J. Chem. Theory Comput.* **2009**, *5*, 962−975.

(18) (a) Belpassi, L.; Infante, I.; Tarantelli, F.; Visscher, L. The chemical bond between Au(I) and the noble gases. Comparative study of NgAuF and $NgAu^+$ (Ng = Ar, Kr, Xe) by density functional and coupled cluster methods. *J. Am. Chem. Soc.* **2008**, *130*, 1048−1060. (b) Bistoni, G.; Rampino, S.; Tarantelli, F.; Belpassi, L. Charge-displacement analysis via natural orbitals for chemical valence: charge transfer effects in coordination chemistry. *J. Chem. Phys.* **2015**, *142*, 084112. (c) Bistoni, G.; Belpassi, L.; Tarantelli, F. Advances in charge displacement analysis. *J. Chem. Theory Comput.* **2016**, *12*, 1236−1244.

(19) The same procedure was successfully employed for studying the H_2 activation with a digermyne complex Zhao, L.; Huang, F.; Lu, G.; Wang, Z.-X.; von Ragué Schleyer, P. Why the mechanisms of digermyne and distannyne reactions with H_2 differ so greatly. *J. Am. Chem. Soc.* **2012**, *134*, 8856−8868.

(20) Jung, Y.; Brynda, M.; Power, P. P.; Head-Gordon, M. Ab initio quantum chemistry calculations on the electronic structure of heavier alkyne congeners: diradical character and reactivity. *J. Am. Chem. Soc.* **2006**, *128*, 7185−7192.

(21) (a) Ziegler, T.; Rauk, A. On the calculation of bonding energies by the Hartree Fock Slater method. *Theor. Chim. Acta* **1977**, *46*, 1−10.

(b) Morokuma, K. Molecular orbital studies of hydrogen bonds. III. C = O···H-O hydrogen bond in H_2CO···H_2O and H_2CO···$2H_2O$. *J. Chem. Phys.* **1971**, *55*, 1236.

(22) (a) Zhao, L.; von Hopffgarten, M.; Andrada, D. M.; Frenking, G. Energy decomposition analysis. *Wiley Interdiscip. Rev.: Comput. Mol. Sci.* **2018**, *8*, No. e1345. (b) Jerabek, P.; Schwerdtfeger, P.; Frenking, G. Dative and electron-sharing bonding in transition metal compounds. *J. Comput. Chem.* **2019**, *40*, 247−264.

https://doi.org/10.1021/jacs.1c06728
J. Am. Chem. Soc. 2021, 143, 14433−14437